

## Distribution of temperature of outgoing flows over the cross-section for different schemes and operating modes of a counterflow vortex tube

© V.N. Samokhvalov

Samara National Research University, Samara, Russia  
E-mail: vn\_samokhvalov@mail.ru

Received June 5, 2024

Revised June 30, 2024

Accepted June 30, 2024

The difference in temperature distributions over the cold and hot air flow cross-sections for the axial and radial arrangements of the counterflow vortex tube outlets has been experimentally established. In the case of axial arrangement of outlets of both the cold and hot air, temperature gradient over the flow cross-section depends on the ratio between the areas of outlet channel cross-sections. The minimum temperature is exhibited by the zones of secondary vortex structures. In the case of radial arrangement of the outlets of both the cold and hot air, temperature over the flow cross-sections evens out due to destruction of secondary large-scale vortex structures.

**Keywords:** vortex tube, temperature separation, vortex structures.

DOI: 10.61011/TPL.2024.10.59705.20013

Inside the energy separation chamber of a counterflow vortex tube (VT), coherent rotating helical structures get formed at the interface between the peripheral and axial flows, which have been studied by various visualization methods [1–6]. Adiabatic cooling occurring due to formation of a near-axis intense vortex core inside the expansion chamber is assumed to be the mechanism for gas cooling in VT [1]. The structure and temperature distribution of the flows leaving VT have been so far studied to a lesser extent. Paper [4] shows that, when the cold gas leaves the VT diaphragm, the secondary vortex core undergoes a complex helical motion.

The goal of the experiments was to study the effect of design arrangement of the counterflow VT outlets (axial or radial) and of the ratio between the outlet opening parameters on the temperature value and distribution over the outgoing flow cross-sections.

The experiments were performed by using a tunable vortex generator (Fig. 1). It allowed us to realize in the experiments the schemes of counterflow VT operation with (i) the axial cold flow outlet and peripheral (radial) hot flow outlet, (ii) counterflow VT operation with axial outlets of both cold and hot flows, and (iii) counterflow VT operation with radial cold flow outlets.

The VT operating modes were switched over by setting/removing plugs on/from its radial (Fig. 1, *a*) or axial (Fig. 1, *b*) outlets. Diameter of the cylindrical VT expansion chamber *I* was 10 mm, its length was 76 mm. The swirler (helices) *2* of the nozzle inlet 2.5 mm thick was constructed based on the Archimedes spiral. Diameters of the fittings' *5–7* openings, as well as those of the cold-air axial outlet openings, were 5.0 mm.

Compressed air at pressure  $P = 0.1–0.6$  MPa was supplied to the vortex tube inlet fitting *5* through a reducer. Air temperature at the VT inlet was  $T_0 = 24^\circ\text{C}$ . Variable

parameters of the experiments were diameter  $d$  of the replaceable diaphragm *3* opening (3.0, 4.0, 4.5 and 5.0 mm) and diameter  $D$  of the replaceable fitting *4* opening (diffuser) (2.5, 3.0, 3.5, 4.0, 5.0 and 6.0 mm). The ratio between the areas of the diaphragm and diffuser openings  $\beta = (d/D)^2$  was taken as a geometric parameter determining the counterflow VT operating mode (relative mass flowrate of the cold flow).

In the case of axial arrangement of the VT outlets, outgoing flows ( $C_A$  is the „cold“ outlet,  $H_A$  is the „hot“ outlet, Fig. 1, *a*) were strongly swirled. To measure the air temperature at various points of the flow cross-section, we used a method of detecting thermal radiation with a thermal imager and temperature transducer in the form of a grid of thin threads made from a low-thermal-conductive material [7]. The temperature transducer grid *8* made from blackened polyamide threads was fixed to the frame (Fig. 1). The grid cell size was  $0.32 \times 0.32$  mm, diameter of longitudinal threads was 0.12 mm, diameter of transverse threads was 0.06 mm. Being arranged in this way, the grid makes the flow gas-dynamic structure disrupted after passing through the grid, but allows fixing the thermal wake of the vortex contacting the grid in this cross-section. Thermographic analysis of the flows was performed using a FLIR SC7000 thermal imaging camera and program code Altair. What was calculated was a decrease in the cold air flow temperature  $\Delta T_C = T_0 - T_i$  ( $\Delta T_{C_A}$  and  $\Delta T_{C_R}$  are the axial and radial outlets, respectively) or variation in the hot air flow temperature  $\Delta T_H = T_i - T_0$  ( $\Delta T_{H_A}$  and  $\Delta T_{H_R}$  are the axial and radial outlets, respectively). Here  $T_i$  is the current temperature at the transformer grid *8* control point.

In the first series of experiments, only axial outlets of the counterflow VT were open (Fig. 1, *a*). At a constant pressure, the VT inlet temperature distribution at different cross-section points of both the flows was quite stable over

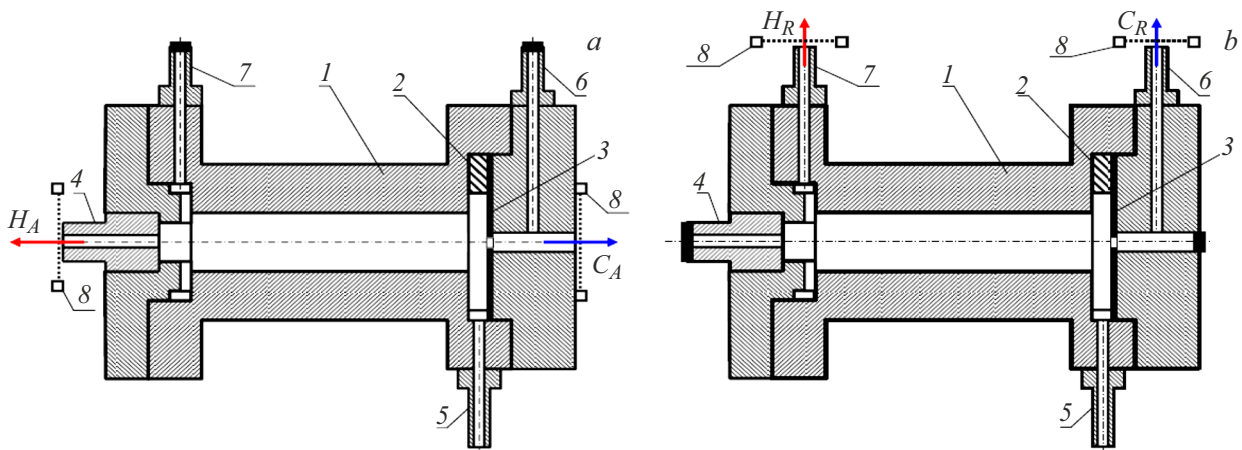


**Figure 1.** Vortex generator layout: *a* — with axial outlets, *b* — with radial outlets. The comments are given in the text.

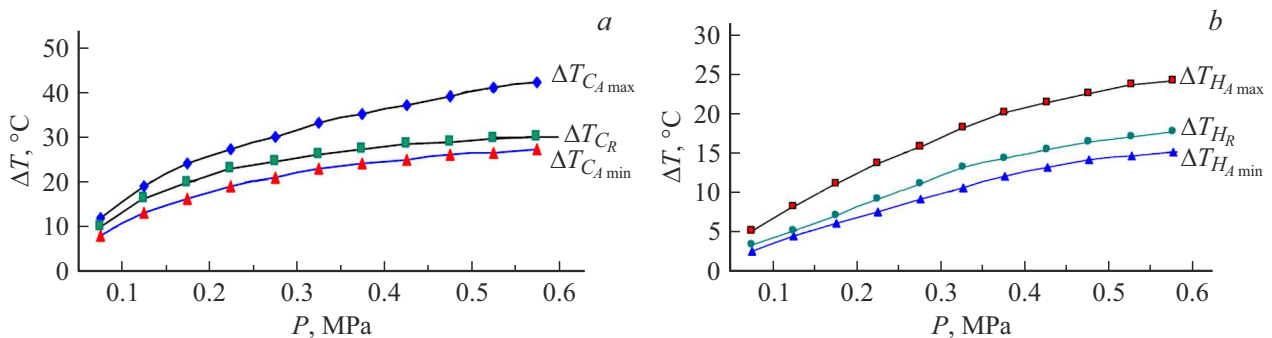


**Figure 2.** Temperature variation versus the VT inlet pressure. *a* — cold air in the axial ( $C_A$ ) and radial ( $C_R$ ) outlet channel ( $\beta = 1.27$ ); *b* — hot air in the axial ( $H_A$ ) and radial ( $H_R$ ) outlet channel ( $\beta = 1.78$ ).

time; however, slight variations in the thermogram pattern was observed. This is obviously due to precession of the coherent vortex structure cores [2–6] in the outgoing air flows.

It was found out that temperatures of both the cold air flow ( $C_A$ ) and hot air flow ( $H_A$ ) at different points of the flow cross-sections can be significantly different at different  $\beta$ . For instance, as the thermograms show,  $\Delta T_{H_A}$  is minus 2–4°C (at  $P = 0.6$ , MPa) at the „hot“ VT axial outlet (flow  $H_A$ ) at  $\beta = 0.25$ –0.44. Cold air occupies almost the entire flow  $H_A$  area (diffuser openings). Here the counterflow VT operates in the mode close to that of the single-flow VT, i.e. as a cooler [8]. As  $\beta$  increases, a thermal „spot“ about  $(1/3$ – $1/2)D$  in diameter is observed in the hot flow thermogram; its temperature is lower than that of the peripheral hot flow. This is obviously a thermal wake of a colder coherent vortex structure coming from the side of the diaphragm [8]. The thermal „spot“ center was shifted from the center of the diffuser opening. The difference between the minimum  $\Delta T_{H_A\min}$  and maximum  $\Delta T_{H_A\max}$  temperatures of the axial flow heating at various flow cross-section points increases with increasing VT inlet pressure (Fig. 2, *b*).

In the „cold“ axial flow  $C_A$  of the vortex tube (Fig. 1, *a*), the difference between the minimum  $\Delta T_{C_A\min}$  and maximum

$\Delta T_{C_A\max}$  cooling at various cross-section points also increases with increasing VT inlet pressure (Fig. 2, *a*). The greatest cooling degree  $\Delta T_{C_A\max}$  of axial flow  $C_A$  occurred at  $\beta = 0.81$ –1. In the case of  $\beta > 1$ , the maximum-cooling zone was located in the central part of flow  $C_A$  (less than  $(1/3)D$  in diameter) but was shifted from the diaphragm cross-section center. The minimum-cooling zone was diametrically opposite to it (Fig. 3). At  $\beta < 0.8$ , on the contrary, the zone of maximum-cooled flow  $C_A$  was located along the periphery of the diaphragm opening. The zone of minimum-cooled flow  $C_A$  was located in the central part of the flow, but was shifted from the diaphragm center. This was obviously caused by hot air inflow from the diffuser.

In the second series of experiments, only radial counterflow VT outlets were open (Fig. 1, *a*). Parameter  $\beta$  was varied by varying diameter  $d$  of the replaceable diaphragm, diameters of the fittings 6 and 7 outlet openings remaining unvaried. Experiments showed that temperature fields of both the cold air flow  $C_R$  and hot air flow  $H_R$  at various flow cross-section points were almost uniform at all values of  $\beta$ . The thermal wake („spot“) of large-scale vortex structures was not observed in the thermogram in both flows over the entire variation range of VT inlet pressure. This is obviously caused by destruction of vortex structures in the hot flow

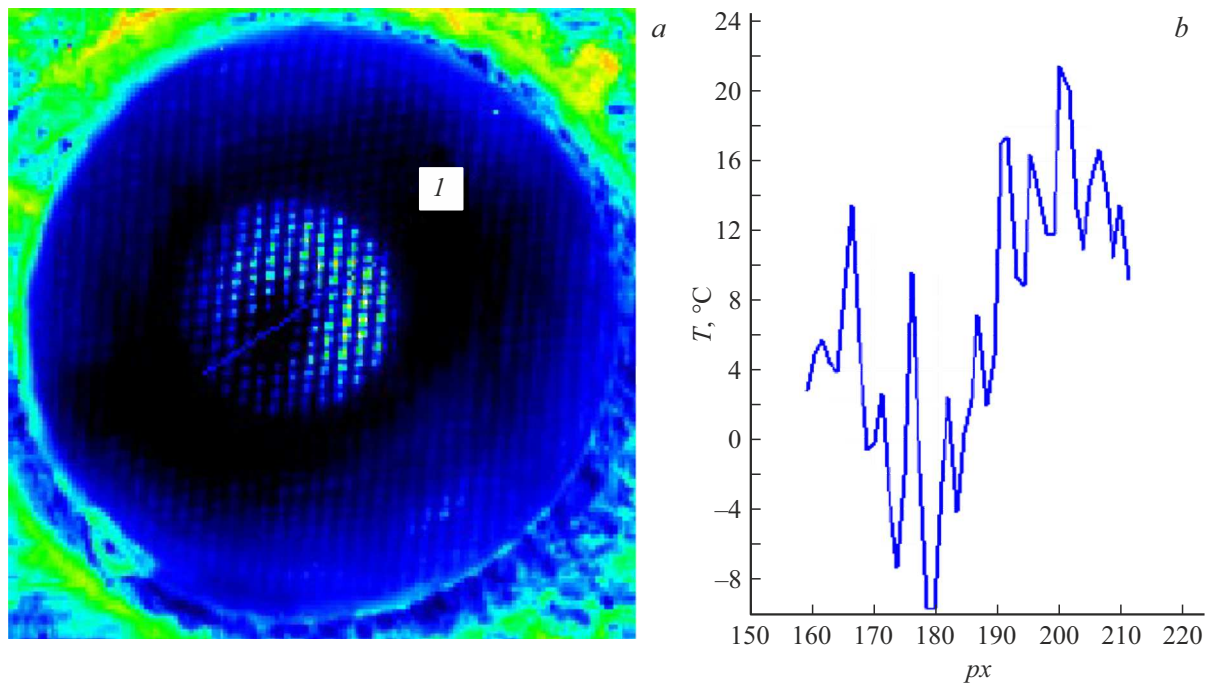


**Figure 3.** Screenshot of the cold flow thermogram, cross-sectional view (a) and temperature distribution along line *I* on the grid (1 px = 0.1 mm,  $d = 4$  mm,  $\beta = 1.78$ ,  $P = 0.6$  MPa) (b).

slit-type deswirler and in the *T*-shaped channel at the cold air flow outlet.

Temperature decrease  $\Delta T_{C_R}$  of cold air leaving through the radial fitting 6 opening was significantly lower than maximum temperature decrease  $\Delta T_{C_{A_{max}}}$  of cold air leaving from the axial opening through diaphragm 3 in the first series of experiments (Fig. 2, a). Increase  $\Delta T_{H_R}$  in the heating temperature of air outgoing through radial fitting 7 (Fig. 1, b) was significantly lower than maximal temperature rise  $\Delta T_{H_{A_{max}}}$  of hot air outgoing through the diffuser (fitting 4 in Fig. 1, a) axial opening in the first series of experiments (Fig. 2, b). Hot air flow  $H_R$  passes to the fitting 7 radial outlet through the slit-type flow deswirler (Fig. 1, a). This leads to destruction of large-scale vortex structures and absence of the thermal „spot“ in the thermogram over the entire range of  $\beta$  and VT inlet pressure and makes heating temperature  $\Delta T_{H_R}$  uniform over the flow  $H_R$  cross-section.

Thus, in a counterflow VT with axial arrangement of the cold and hot air outlets, with the ratio between the areas of diaphragm and diffuser openings  $\beta < 1$ , a significant temperature gradient gets formed over the outgoing hot flow cross-section, which increases with decreasing  $\beta$  due to cold air inflow from the diaphragm. In the cross-section of the outgoing cold flow, the greatest degree of air cooling was observed at  $\beta = 0.81-1$  and decreased with increasing  $\beta$  due to the hot air inflow from the diffuser with simultaneous increase in the temperature gradient over the flow cross-section. In the case of radial arrangement of the counterflow VT outlets of cold and hot air, the temperature gradient

over the flow cross-sections is almost fully absent because of destruction of secondary vortex structures.

### Conflict of interests

The author declares that he has no conflict of interests.

### References

- [1] V.A. Arbuzov, Yu.N. Dubnishchev, A.V. Lebedev, M.Kh. Pravdina, N.I. Yavorski, *Tech. Phys. Lett.*, **23** (12), 938 (1997). DOI: 10.1134/1.1261939.
- [2] Yu.M. Akhmetov, E.I. Zangirov, A.V. Svistunov, *Tr. MFTI*, **6** (2), 99 (2014). (in Russian)
- [3] X. Guo, B. Zhang, B. Liu, X. Xu, *Int. J. Refrig.*, **104** (6), 51 (2019). DOI: 10.1016/j.ijrefrig.2019.04.030
- [4] Sh.A. Piralishvili, *Vikhrevoy effekt* (Nauchtekhlitizdat, M., 2013), t. 1. (in Russian)
- [5] Y. Xue, J.R. Binns, M. Arjomandi, H. Yan, *Int. J. Heat Fluid Flow*, **75** (2), 195 (2019). DOI: 10.1016/j.ijheatfluidflow.2019.01.005
- [6] X. Guo, B. Liu, B. Zhang, Y. Shan, *Int. J. Therm. Sci.*, **168**, 107067 (2021). DOI: 10.1016/j.ijthermalsci.2021.107067
- [7] B.P. Zhilkin, I.D. Larionov, A.N. Shuba, *Instrum. Exp. Tech.*, **47** (4), 545 (2004). DOI: 10.1023/B:INET.0000038406.76066.35.
- [8] V.N. Samokhvalov, *Tech. Phys. Lett.*, **48** (1), 12 (2022). DOI: 10.1134/S1063785022010059.

*Translated by EgoTranslating*